EVALUATION OF ECONOMIC IMPACT OF RENEWABLE WIND ENERGY AND ESS INTEGRATION USING MULTIPERIOD OPTIMAL POWER FLOW

Andaluri Manindra[1], Prof. K. Vaisakh[2]

Department of Electrical Engineering, Andhra University, Visakhapatnam, AP

Abstract: *This paper presents a Multi-Period AC Optimal Power Flow (AC-OPF) model that integrates renewable wind energy and Energy Storage Systems (ESS) to address the challenges of intermittent and variable renewable energy sources in modern power systems. The model is implemented using the General Algebraic Modelling System (GAMS) and tested on a benchmark power system. By considering the multi-period nature of wind power generation and the operational flexibility ESS provides, the optimization framework aims to minimize total generation costs while satisfying power system constraints, including power balance, voltage limits, thermal limitations, and ESS operational limits.*

The integration of wind energy introduces variability and uncertainty, which are effectively managed by strategically deploying ESS to store surplus energy and provide additional capacity during deficits. Simulation results demonstrate that combining wind energy and ESS reduces reliance on conventional generation, enhances system reliability, and improves cost efficiency. The study provides valuable insights into the role of advanced optimization techniques in enabling the transition to renewable and sustainable power systems.

Keywords*:* **Multi-Period AC Optimal Power Flow (AC-OPF), General Algebraic Modelling System (GAMS), Energy storage system (ESS).**

1. INTRODUCTION

The increasing penetration of renewable energy sources (RES) in modern power systems is a key step toward achieving global energy sustainability and reducing greenhouse gas emissions. Among RES, wind energy has emerged as one of the most promising technologies due to its abundance and cost-effectiveness. However, the inherent variability and intermittency of wind generation pose significant challenges to the reliable and economic operation of power systems. To address these challenges, Energy Storage Systems (ESS) have been identified as a crucial component in ensuring system flexibility and stability. ESS can effectively store surplus energy during periods of high wind generation and supply energy during low wind conditions, thus mitigating the imbalance between supply and demand. The Multi-Period Alternating Current Optimal Power Flow (AC-OPF) problem provides a comprehensive framework for modelling and optimizing power system operations over successive time periods. By incorporating wind energy and ESS into the AC-OPF framework, power system operators can better manage the variability of renewable resources while minimizing operational costs and maintaining system reliability [1]. The multi-period approach captures temporal dependencies, such as the state of charge of ESS and the fluctuations in wind power, enabling a more realistic and practical optimization.

This paper develops a Multi-Period AC-OPF model that integrates wind energy and ESS, implemented using the General Algebraic Modelling System (GAMS). The proposed model

aims to minimize total generation costs while ensuring compliance with system constraints, including power balance, voltage stability, thermal limits, and ESS operational requirements.[2] Multi period AC optimal power flow (AC-OPF) problem is implemented for a dynamic load in 24 hours is solved using 3 different cases, Case1-Load shedding with 12 generators is implemented, Case-2 thermal with the wind integration, Case3 thermal with 2 Energy Storage Systems at bus 19 and 21. All the cases are solved using nlp (nonlinear programming) in GAMS software.

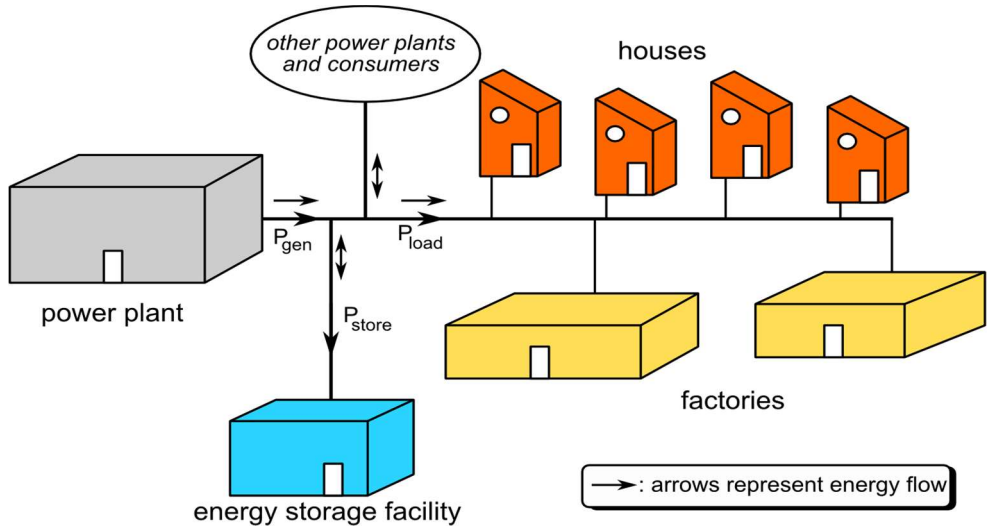

Fig.1. Energy storage System Connected to Grid

Several studies have focused on investigating the suitability and selection of optimal energy storage systems for specific applications. [3-4] Literature reviews compile existing information on state-of-the-art technologies and compare their uses based on current projects. Some studies go further by evaluating and ranking different energy storage systems using multi-criteria decision analysis. Another approach model's storage as equivalent circuits to assess its performance, while an indexing method has been suggested in some studies, although it remains in the early stages. To maximize the economic potential of grid-connected energy storage systems, it is beneficial to consider a portfolio approach that combines multiple services for one or more applications.[5] This strategy allows a single storage system to generate several revenue streams, thus improving its utilization. For example, combining frequency response with reserve services or integrating load peak shaving with power smoothing has been explored.

2. LITERATURE REVIEW

The transition toward renewable energy has been widely documented in the literature. Several studies emphasize the role of wind energy in reducing the dependency on fossil fuels. For example, Smith et al. (2020) demonstrated that integrating wind energy reduces overall carbon emissions while improving cost efficiency. Similarly, Brown and Green (2021) explored the economic implications of adding ESS to power systems, highlighting their ability to address the intermittency of renewable sources.

Despite these advancements, limited research has focused on multi-period optimization models that consider dynamic power flow over time. Existing models often lack the ability to

incorporate real-time variations in renewable energy generation. This paper bridges this gap by introducing a multi-period AC-OPF model that optimally dispatches generation resources while addressing both technical and economic constraints.

3. MODELLING ENERGY STORAGE SYSTEMS

ESS is added at bus 19 and bus 21 with capacities 200MW and 100MW respectively. State of charge of ESS is formulated in equation (1)

$$SOC_{i,t} = SOC_{i,t-1} + P^{c}_{i,t}\eta_c - \frac{P^{d}_{i,t}}{\eta_d} \quad (1)$$

In the above equation $SOC_{i,t}$ is State of Charge for ESS at i^{th} and time t, $SOC_{i,t}$ is State of Charge for ESS at i^{th} and an hour before time t. Charging efficiency is 95% and discharging efficiency is 90%. ESS charging and discharging limits are formulated in equations (2) and (3)

$$P^{c}_{i,min} < P^{c}_{i,t} < P^{c}_{i,max} \quad (2)$$

$$P^{d}_{i,min} < P^{d}_{i,t} < P^{d}_{i,max} \quad (3)$$

In the equation (2) and equation (3) $P^{c}_{i,t}$ is real charging power of ESS connected to i^{th} bus at time t, $P^{d}_{i,t}$ real discharging power of ESS connected to i^{th} bus at time t.$P^{c}_{i,max}$ is the maximum capacity of ESS connected to i^{th} bus and $P^{c}_{i,min}$ is the minimum capacity of ESS connected to i^{th} bus. since this have 2 ESS at bus 19 and bus 21, at bus at 19 $P^{c}_{i,min}$ is 0MW and $P^{c}_{i,max}$ is 200MW and for ESS at bus 21 $P^{c}_{i,min}$ is 0MW and $P^{c}_{i,max}$ is 100MW.[6-8]

Considering Dynamic pricing system, the charging and discharge price of ESS varies continuously the values of ESS charging and discharge price are taken for a case of minimizing grid investment. Since charging is considered as load and discharge is considered as source for charging costumer needs to pay to the grid whereas for discharge grid pays to the ESS station.

4. PROBLEM FORMULATION

Multi-Period Optimal AC Power Flow:

4.1 Power flow equations:

The active and reactive power flows in each branch connecting bus i to bus j in the AC network are specified as follows.

$$P_{ij,t}=\text{real}\ \{S_{ij,t}\} = \frac{V^{2}_{i,t}}{Z_{ij}}\cos\theta_{ij} - \frac{V_{i,t}V_{j,t}}{Z_{ij}}\cos(\delta_{i,t} - \delta_{j,t} + \theta_{ij}) \quad (4)$$

$$Q_{ij,t}=\text{img}\ \{S_{ij,t}\} = \frac{V^{2}_{i,t}}{Z_{ij}}\sin\theta_{ij} - \frac{V_{i,t}V_{j,t}}{Z_{ij}}\sin(\delta_{i,t} - \delta_{j,t} + \theta_{ij}) - \frac{bV^{2}_{i,t}}{2} \quad (5)$$

Here $S_{ij,t}$ is the apparent power from the bus i to bus j , $V_{i,t}V_{j,t}$ are voltages of i^{th} and j^{th} bus in per units respectively. Z_{ij} is the impedance between i^{th} and j^{th} bus.

4.2 Objective function:

The objective function (OF) is fuel cost of thermal generation, the objective is to minimize the OF over the scheduled time horizon of 24hours:

$$OF = \sum_{i,t}^{i=24,t=24} b_g(P_{i,t}^g) \quad (6)$$

Here, b_g *is the* Fuel cost coefficient of active power at thermal generating unit and $P_{i,t}^g$ is real power generation at g^{th} thermal unit at bus i and time t

4.3 Power balance constraint

$$P_{i,t}^g + P_{i,t}^s - P_{i,t}^l - P_{i,t}^c + P_{i,t}^d = \sum P_{ij,t} \quad (7)$$

$$Q_{i,t}^g - Q_{i,t}^l = \sum Q_{ij,t} \quad (8)$$

Here, $P_{i,t}^l$ is the Active power demand on bus i at time t, $P_{i,t}^s$ is the Solar active power at bus i and time t, $P_{i,t}^c$ Real charging power of ESS at bus i and time t, $P_{i,t}^d$ Real discharging power of ESS at bus i and time t and $\sum P_{ij,t}$ is the real power loss at time t $Q_{i,t}^g$ is reactive power generation at g^{th} thermal unit at bus i and time t,$Q_{i,t}^l$ is reactive power demand on bus i at time t and $\sum Q_{ij,t}$ is the reactive power loss at time t.

4.4 Generator limit constraints

$$-S_{ij}^{max} < S_{ij,t} < S_{ij}^{max} \quad (9)$$

$$P_i^{g,min} < P_{i,t}^g < P_i^{g,max} \quad (10)$$

$$Q_i^{g,min} < Q_{i,t}^g < Q_i^{g,max} \quad (11)$$

Here, S_{ij}^{max} is the maximum apparent power flow from i^{th} and j^{th} bus. $P_i^{g,max}$ is the maximum real power generation of g^{th} thermal unit at bus i. $P_i^{g,min}$ is the minimum real power generation of g^{th} thermal unit at bus i. $Q_i^{g,max}$ is the maximum reactive power generation of g^{th} thermal unit at bus i. $Q_i^{g,min}$ is the minimum reactive power generation of g^{th} thermal unit at bus i.

4.5 Ramp up and ramp down constraints:

$$P_{i,t}^g - P_{i,t-1}^g < RU_g \quad (12)$$

$$P_{i,t-1}^g - P_{i,t}^g < RD_g \quad (13)$$

For thermal generation ramp rate constraints for each unit, output is limited by ramp up or ramp down rate at each hour. In the above equations RU_g is the ramp up value of thermal generator g connected to i^{th} bus and RD_g ramp down value of thermal generator g connected to i^{th} bus. [9-11]

5. METHODOLOGY

The Multiperiod AC Optimal Power Flow (AC-OPF) problem is a complex optimization task that aims to optimize the operation of power systems over a defined time horizon while adhering to system constraints. This methodology incorporates the integration of Energy Storage Systems (ESS) and solar energy, highlighting their impact on the operation of thermal units. The process is implemented using the General Algebraic Modelling System (GAMS) with the Nonlinear Programming (NLP) solver. The detailed steps involved are as follows:

Steps involved in Multiperiod AC-OPF Process:

5.1 Problem Setup and Definitions

a) Sets:

- Time Steps: The 24-hour planning horizon is divided into discrete time intervals, t∈{1,2,3,…,24}t \in \{1, 2, 3, \ldots, 24\}t∈{1,2,3,…,24}, to model the dynamic behaviour of load demand and generation over the day.
- Buses: The IEEE 24-bus test system is used, where i∈{1,2,3,…,24}i \in \{1, 2, 3, \ldots, 24\}i∈{1,2,3,…,24} represents buses in the network. Generating buses, load buses, and buses with ESS are defined as subsets.
- Generators: Generating units g∈{1,2,…,12}g \in \{1, 2, \ldots, 12\}g∈{1,2,…,12} are mapped to specific buses based on their locations.

b) Tables:

- Generator Parameters: Tables include data on thermal generator capacities, costs, fuel consumption rates, and ramping limits.
- Dynamic Load Data**:** Hourly variations in load demand are modelled and provided in tabular form.
- Line Data**:** Information on transmission line impedance, capacity, and connectivity between buses is incorporated to model power flow constraints.

5.2 Variables

- Generator Outputs: Variables include the real power ($P_{g,t}$) and reactive power ($Q_{g,t}$) outputs of thermal generators at each time step.
- State of Charge (SoC): The state of charge of ESS ($SoC_{i,t}$) is modelled as a time-dependent variable to capture charging and discharging dynamics.
- Voltage and Phase Angles: Voltage magnitudes (V_i) and phase angles (θ_i) at each bus are treated as variables to solve the AC power flow equations.

5.3 Scalars

- Fixed quantities, such as ESS efficiency, capacity limits, and the initial SoC, are defined using scalar variables. For instance:
- ESS charging and discharging efficiency (η_c,η_d).

- ESS capacity (C_{ESS}).
- Initial state of charge ($SoC_{i,0}$).

5.4 Equations

a) Power Balance Equations:

- At each bus and for each time step, the total power generation, load demand, ESS operation, and network losses are balanced:

$$P_{g,t} + P_{ESS,t} = P_{load,t} + P_{loss,t} \quad (14)$$

b) AC Power Flow Equations:

- The nonlinear relationship between bus voltages, phase angles, and power flow is modelled using the AC power flow equations:

$$P_{ij} = V_i V_j (G_{ij} cos(\theta_i - \theta_j) + B_{ij} sin(\theta_i - \theta_j))) \quad (15)$$

$$Q_{ij} = V_i V_j (G_{ij} cos(\theta_i - \theta_j) - B_{ij} sin(\theta_i - \theta_j))) \quad (16)$$

c) ESS Operational Constraints:

- ESS charging and discharging are governed by the following constraints:

$$SoC_{i,t} = SoC_{i,t-1} + \eta_c P_{ch,i,t} - \frac{P_{ch,i,t}}{\eta_d} \quad (17)$$

$$0 \leq SoC_{i,t} \leq CESS \quad (18)$$

d) Generator Ramping Constraints:

- Thermal generators are subject to ramping limits to ensure smooth transitions between consecutive time steps:

$$| P_{g,t} - P_{g,t-1} | \leq R_g \quad (19)$$

e) Voltage and Line Flow Limits:

- Bus voltage magnitudes and line flows are maintained within specified operational limits:

$$| P_{ij} | \leq P_{ij,max} \quad (20)$$

$$V_{min} \leq V_i \leq V_{max} \quad (21)$$

5.5 Modelling and Solver Implementation

a) Model Formulation:

- The equations are combined to form a comprehensive optimization problem using the model keyword in GAMS. The objective function minimizes the total operational cost:

$$Minimize: \sum_t \sum_g C_g P_{g,t} + \sum_i C_{ESS} (Pch, i, t + P_{ch,i,t} + P_{dis,i,t}) \quad (22)$$

where C_g and C_{ESS} represent cost coefficients for generators and ESS operation, respectively.

b) **Solver Configuration:**

- The NLP solver is employed to handle the nonlinear nature of the AC power flow equations. Solver parameters, such as convergence tolerance and iteration limits, are fine-tuned for efficient computation.

5.6 Output Extraction

The solution, including generator outputs, ESS states, bus voltages, and line flows, is extracted from the GDX file generated by GAMS. These results are analyzed to assess the impact of ESS and solar integration on the operation of thermal units.

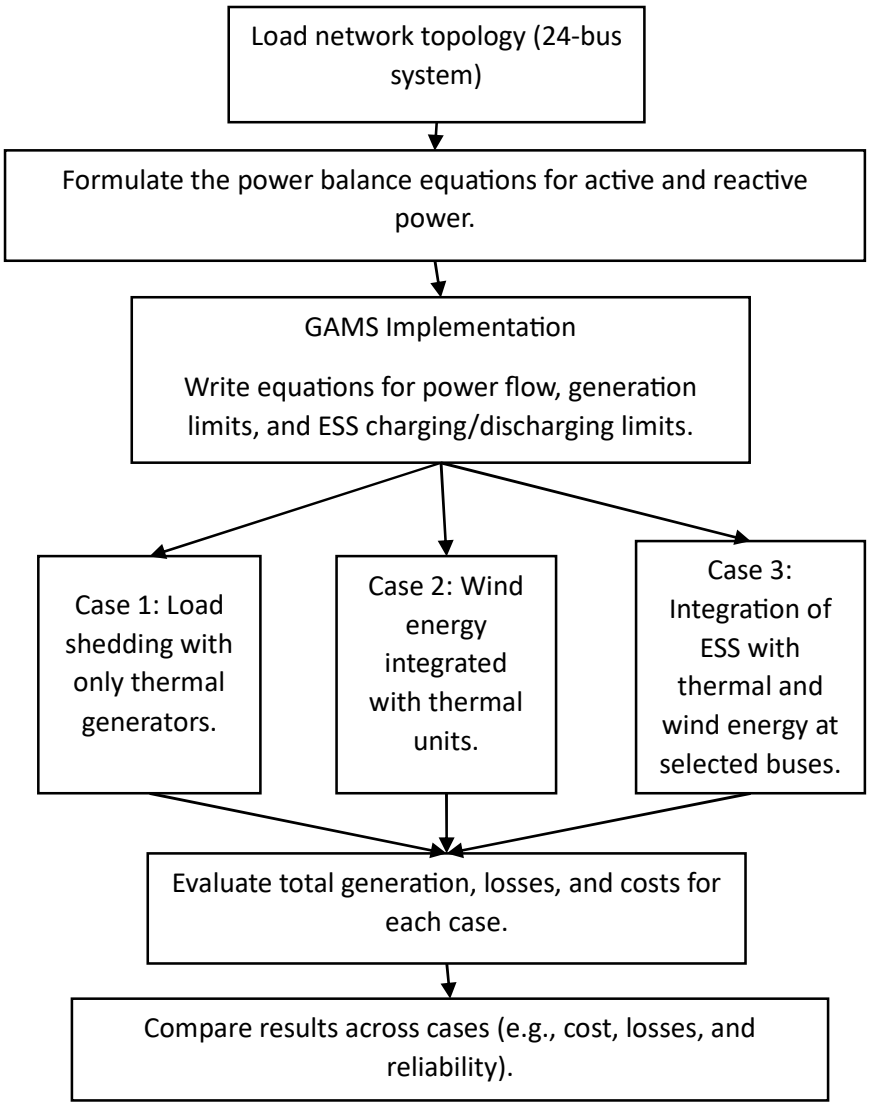

Fig.2. Step-by-Step Framework for Power System Optimization and Analysis

6. RESULTS AND DISCUSSIONS

The IEEE RTS 24-bus network, Information about 12 thermal generating units is given in Table 1. It is a transmission network with the voltage levels of 138kV, 230kV and Sbase = 100MVA. Three ESS are installed, each with the capacity of 100 MW ,150MW and 200 Mw are connected to busses 8,19 and 21 respectively and also wind capacities same as that the ESS capacities.

Table 1. Parameters of thermal generating units

Generating BUS	P_g^{max} (MW)	P_g^{min} (MW)	b_g ($/MW)	Q_g^{max} (Mvar)	Q_g^{min} (Mvar)	RU (MW/h)	RD (MW/h)
1	152	30.4	13.32	60	-50	21	21
2	152	30.4	13.32	60	-50	21	21
7	300	75	20.7	180	0	43	43
13	591	207	20.93	240	0	31	31
15	215	66.30	21	110	-50	28	28
16	155	54.30	10.52	80	-50	31	31
18	400	100	5.47	200	-50	70	70
21	400	100	5.47	200	-50	70	70
22	300	60	0	96	-60	53	53
23	660	248.4	10.52	310	-125	49	49

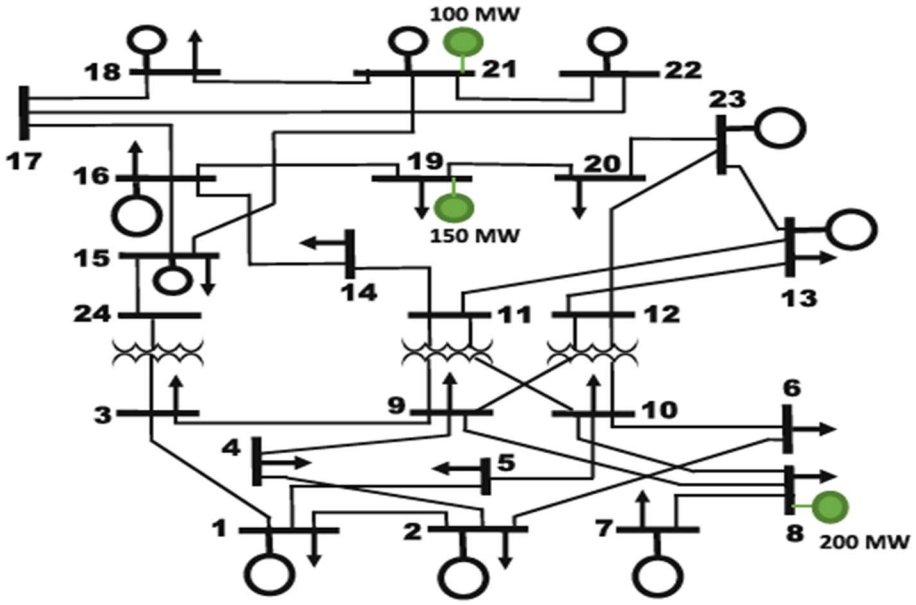

Fig 3. IEEE wind connection to network integration

Table 2. Branch data for IEEE 24 BUS Test System

From	To	r (p.u)	x (p.u)	b (p.u)	Limit
1	2	0.0026	0.0139	0.4611	175
1	3	0.0546	0.2112	0.0572	175
1	5	0.0218	0.0845	0.0229	175

2	4	0.0328	0.1267	0.0343	175
2	6	0.0497	0.192	0.052	175
3	9	0.0308	0.119	0.0322	400
3	24	0.0023	0.0839	0	175
4	9	0.0268	0.1037	0.0281	175
5	10	0.0228	0.0883	0.0239	175
6	10	0.0139	0.0605	2.459	175
7	8	0.0159	0.0614	0.0166	175
8	9	0.0427	0.1651	0.0447	175
8	10	0.0427	0.1651	0.0447	175
9	11	0.0023	0.0839	0	400
9	12	0.0023	0.0839	0	400
10	11	0.0023	0.0839	0	400
10	12	0.0023	0.0839	0	400
11	13	0.0061	0.0476	0.0999	500
11	14	0.0054	0.0418	0.0879	500
12	13	0.0061	0.0476	0.0999	500
12	23	0.0124	0.0966	0.203	500
13	23	0.0111	0.0865	0.1818	500
14	16	0.005	0.0389	0.0818	500
15	16	0.0022	0.0173	0.0364	500
15	21	0.00315	0.0245	0.206	1000
15	24	0.0067	0.0519	0.1091	500
16	17	0.0033	0.0259	0.0545	500
16	19	0.003	0.0231	0.0485	500
17	18	0.0018	0.0144	0.0303	500
17	22	0.0135	0.1053	0.2212	500
18	21	0.00165	0.01295	0.109	1000
19	20	0.00225	0.0198	0.1666	1000
20	23	0.0014	0.0108	0.091	1000
21	22	0.0087	0.0678	0.1424	500

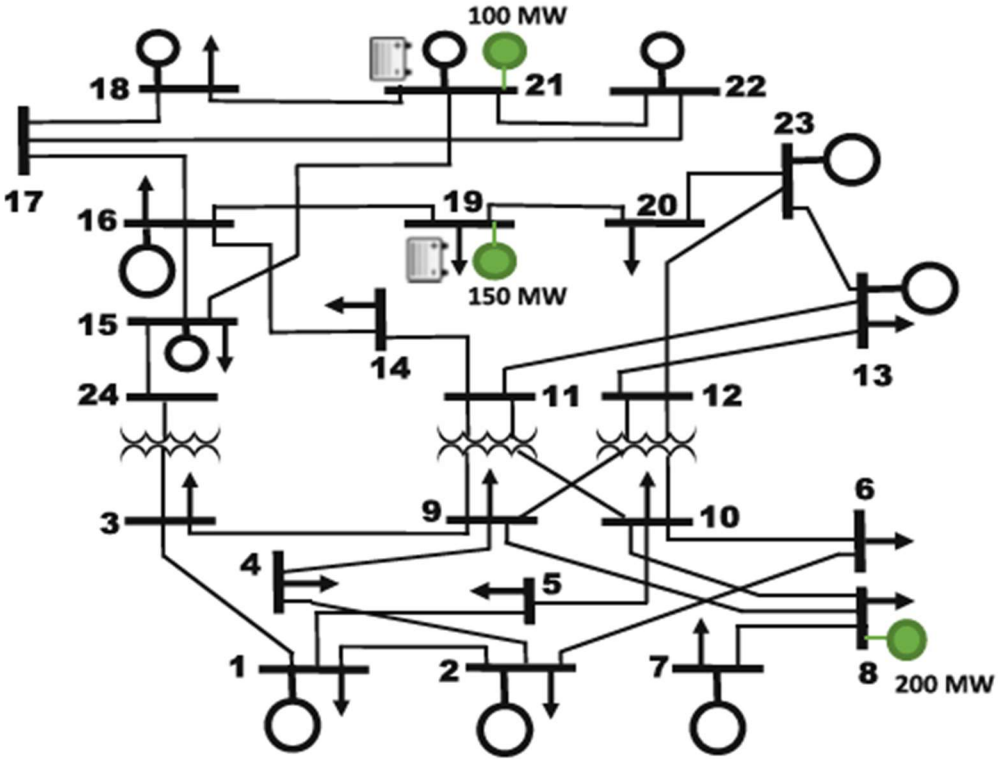

Fig.4. The IEEE 24 RTS with ESS integration

In Fig.3, the focus is on integrating wind energy into the IEEE 24-bus system. Wind power sources are added to specific buses, including a 100 MW unit and a 150 MW unit, to contribute renewable energy to the grid. This setup demonstrates how wind energy is incorporated into the existing infrastructure to enhance power generation capacity and reduce reliance on conventional sources.

In Fig.4. the system is further enhanced by integrating energy storage systems (ESS) alongside the wind power sources. These storage units are strategically placed near the wind farms to store surplus energy generated during low-demand periods and release it during peak demand. This configuration highlights the combined benefits of renewable energy and storage, ensuring improved grid flexibility, reliability, and efficiency in managing energy supply and demand.

Results are obtained for the Multiperiod AC- optimal power flow (AC-OPF) problem is implemented for a dynamic load in 24 hours is solved in three different cases, Case1-Load shedding with 12 generators is implemented, Case-2 thermal with the wind integration, Case3 thermal with 2 Energy Storage Systems at bus 19 and 21. All the cases are solved using NLP (nonlinear programming) in GAMS software.

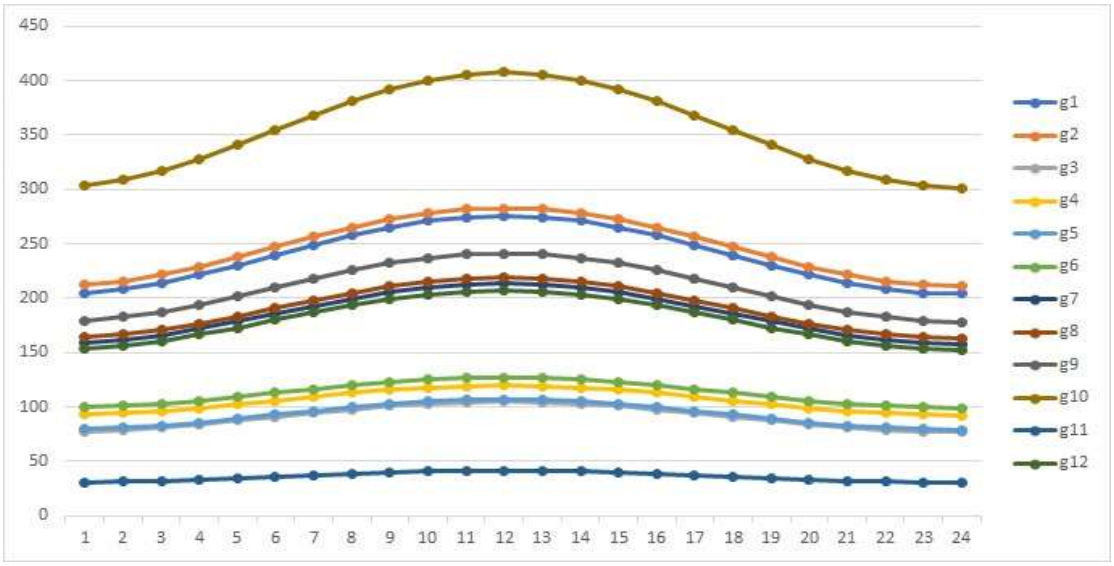

Fig. 5. Optimal Active power generation of thermal units in MP-ACOPF (Only Thermal Units) case1

Fig.5. shows the total demand variation in megawatts (MW) over 24 hours for Case 1, where load shedding is implemented using 12 generators. The demand follows a typical diurnal pattern, starting low during early hours, increasing steadily throughout the day, peaking around mid-day, and then gradually decreasing in the evening. This variation provides the basis for scheduling generation units dynamically to meet demand.

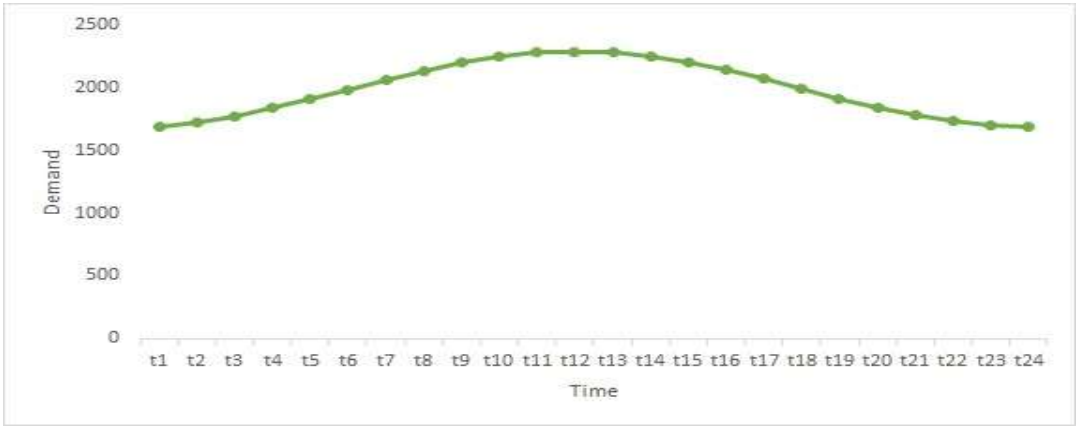

Fig.6.Demand in Mw variation on system w.r.t time in case 1

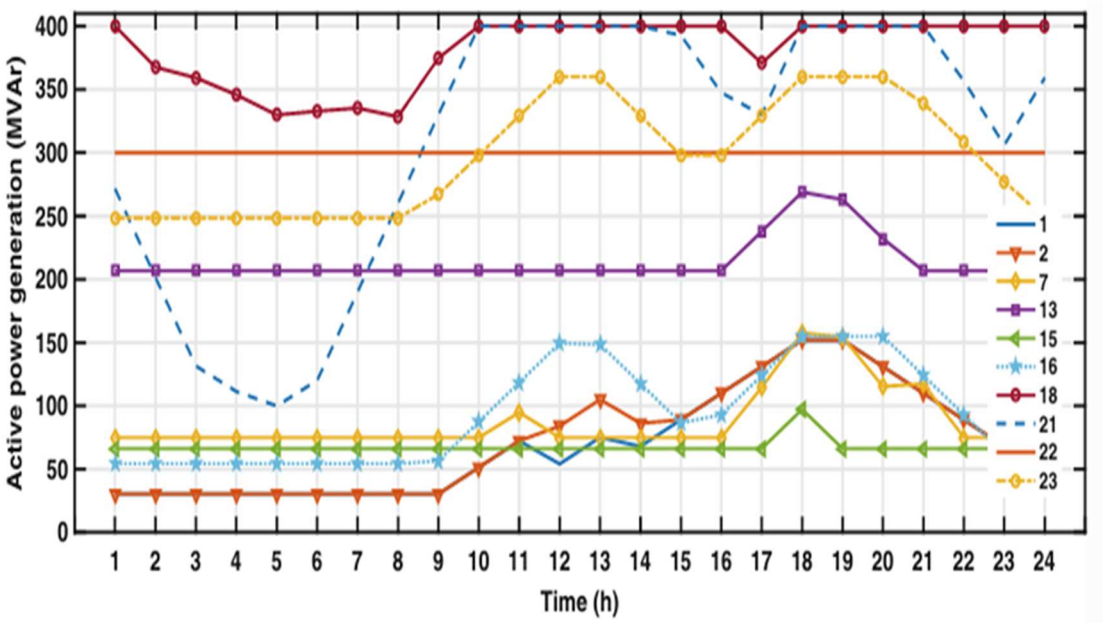

Fig.7.Active power generation of thermal units in MP-AC OPF in case-2

Fig.6. illustrates the optimal active power generation of thermal units under Case 1 for MP-OPF. Each generator's power output is plotted over 24 hours, showing how the units are dispatched to meet demand while minimizing costs or losses. Some generators operate at relatively constant levels (likely base load units), while others adjust their output significantly, reflecting their role in handling peak or variable demands.

Fig.7. depicts the active power generation of thermal units in Case 2, where wind integration is added to the system. The power outputs of different thermal generators are shown over 24 hours, highlighting the system's operational adjustments with renewable energy contributions. Thermal units with flexible outputs adjust more frequently to accommodate the variability of wind power. Certain generators may have reduced output, reflecting the substitution of renewable energy for thermal generation to meet the overall demand efficiently.

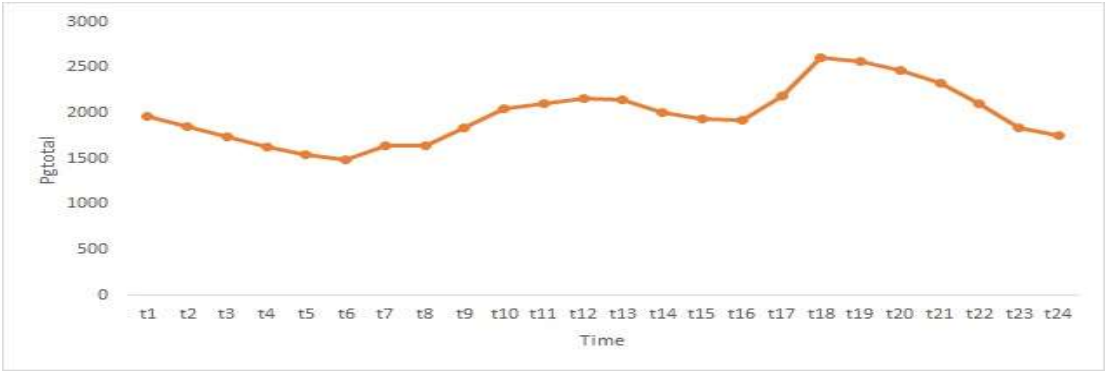

Fig .8. Total thermal power generation to meet demand and losses in case-2

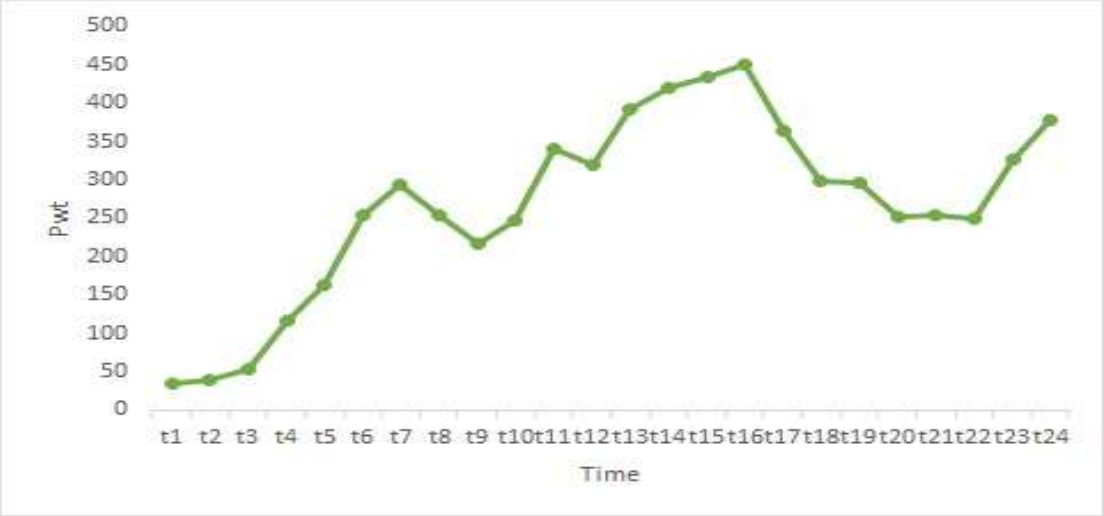

Fig .9. Total wind power generation in case-2

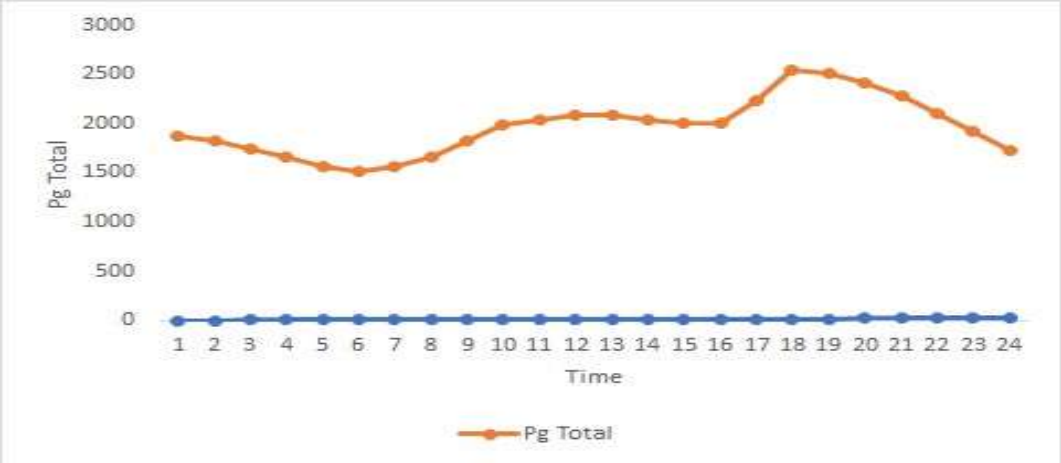

Fig .10. Total Power Generation to meet demand and losses in case-3

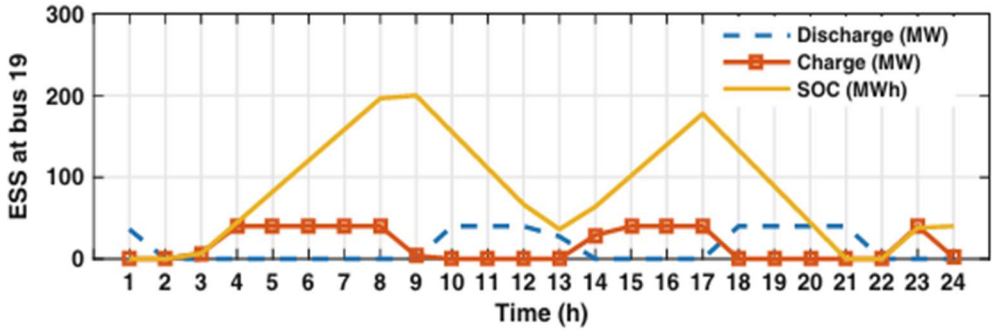

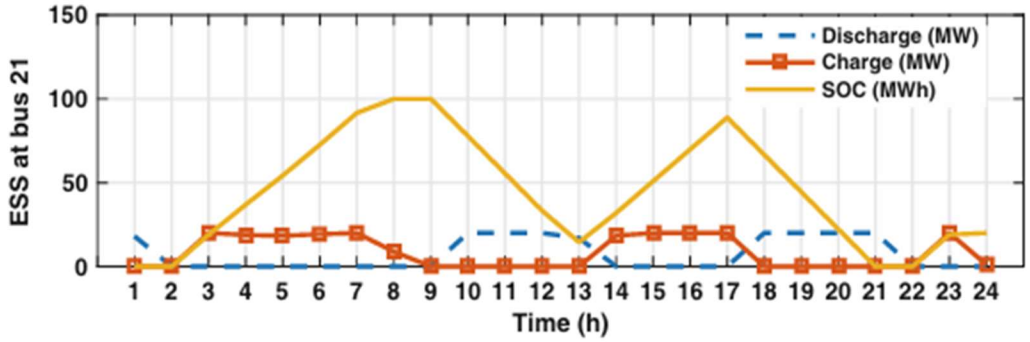

Fig.11. The hourly dispatch of ESS in case-3

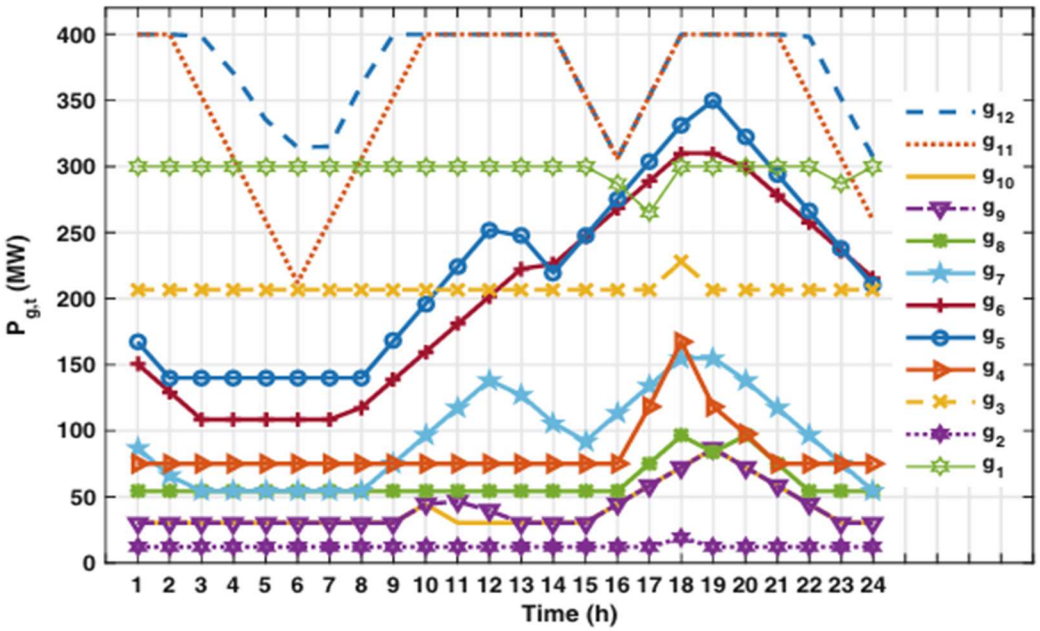

Fig .12. The hourly dispatch of all the 12 generators in case-3

Fig.11. shows the total power generation (P_{wt}) over time, measured in hours from t1 to t24. It illustrates how the total power generated fluctuates throughout the day to meet both demand and system losses. Initially, power generation is low, gradually increasing during the day, peaking between t15 and t18, and then declining before rising slightly again towards the end of the day.

Fig.12. depicts the hourly power dispatch of 12 generators. Some generators, like g12, operate consistently at high capacities, likely covering the base load, while others, such as g9 and g11 , ramp up significantly during peak demand hours. Meanwhile, generators like g1g and g2, contribute minimally or maintain consistent outputs, possibly serving as reserves or supporting specific tasks. Together, these graphs highlight how the system dynamically distributes generation to balance demand and optimize daily performance.

Table 2. Total power generation and demand of all cases

Case-1		Case -2		Case -3	
Pgt	**Demand**	**Pgt**	**Demand**	**Pgt**	**Demand**
1711.222	1710.222	1999.338	1950.857	1880.23	1830.23
1742.192	1740.192	1883.974	1835.75	1820.56	1772.56
1790.868	1787.868	1790.093	1747.247	1740.65	1828.65
1856	1850	1745.683	1709.24	1660.85	1648.85
1927.354	1922.354	1710.594	1678.299	1570.63	1563.63
2006	2000	1734.506	1704.353	1510.32	1576.32
2085.646	2077.646	1818.594	1786.34	1560.41	1621.41
2158	2150	1893.836	1857.468	1660.23	1771.23
2224.132	2212.132	2056.761	2012.212	1820.96	1919.96
2269.808	2259.808	2292.641	2242.97	1980.52	2085.52
2302.778	2289.778	2445.231	2391.198	2030.78	1926.78
2310	2300	2481.981	2430.93	2090.87	1980.87
2302.778	2287.778	2535.236	2481.33	2080.91	2229.91
2273.808	2259.808	2430.85	2377.624	2040.15	2114.15
2227.132	2212.132	2373.695	2327.129	2000.38	2197.38
2166	2150	2376.542	2335.275	2000.74	1980.74
2090.646	2077.646	2551.34	2491.103	2230.67	2114.67
2018	2000	2902.804	2850	2550.97	2771.97
1934.354	1922.354	2854.378	2803.305	2510.58	2579.58
1859	1850	2722.653	2668.651	2420.62	2438.62
1800.868	1787.868	2583.831	2529.653	2280.12	2172.12

In Case-1, the power generation (Pgt) is closely matched to the demand across all rows, with minimal differences between the two values. This balance indicates efficient management of resources, likely resulting in stable costs.

In Case-2, the demand generally lags behind power generation, especially in higher rows (e.g., row 1: Pgt = 1999.338, Demand = 1950.857). This surplus of power generation can lead to increased operational costs because the generated power is underutilized. For Case-3, the demand frequently exceeds power generation (e.g., row 18: Pgt = 2550.97, Demand = 2771.97).

This deficit suggests reliance on backup power sources or costly external procurement, leading to higher costs. The power generation in Case-1 is efficient and closely balanced with demand, minimizing both the risk of shortages and excess generation.

Table 3. Cost estimation of all cases

Parameters	Load shedding	Thermal with Wind energy integration	Thermal with ESS
Total fuel cost ($)	263878.17	435925.894	498204.802
Total power generation (MW)	48241	53834.976	47203.9
Total power loss (MW)	243	1101.099	1174

Table 3 provides a comparative analysis of cost and performance metrics for three power generation strategies: Load Shedding, Thermal with Wind Energy Integration, and Thermal with Energy Storage System (ESS). The total fuel cost is lowest for Load Shedding at $263,878.17, reflecting its cost-effectiveness but limited capacity to meet demand. In contrast, Thermal with Wind Energy Integration incurs a moderate fuel cost of $435,925.89 due to the partial reliance on renewable energy, while Thermal with ESS has the highest cost at $498,204.80, driven by the added expenses of storage systems and thermal plant operations.

In terms of total power generation, the Thermal with Wind Energy Integration case achieves the highest output at 53,834.976 MW, benefiting from the additional capacity provided by wind energy. Load Shedding generates the least at 48,241 MW, as it deliberately reduces output during peak demand. Thermal with ESS generates 47,203.9 MW, with storage ensuring energy availability despite slightly lower generation levels.

Regarding total power loss, Load Shedding exhibits the least loss at 243 MW, as reduced generation minimizes transmission and distribution inefficiencies. Thermal with Wind Energy Integration records higher losses of 1,101.099 MW, largely due to integration challenges associated with renewable energy. Thermal with ESS has the highest losses at 1,174 MW, likely resulting from storage inefficiencies and the complexity of combined system operations. This analysis highlights the trade-offs between cost, generation capacity, and efficiency for each strategy, aiding stakeholders in selecting an approach that balances economic and operational priorities.

7. CONCLUSION

This paper has presented a Multi-Period AC Optimal Power Flow (AC-OPF) framework that integrates renewable wind energy and Energy Storage Systems (ESS) to address the challenges posed by renewable energy variability and intermittency. Implemented using the General Algebraic Modeling System (GAMS), the proposed model optimizes power system operations across multiple time periods, minimizing total generation costs while satisfying system constraints such as power balance, voltage limits, and ESS operational requirements.

The results demonstrate the significant benefits of incorporating ESS alongside wind energy in modern power systems. ESS effectively mitigates the impact of wind generation variability by storing excess energy during periods of high wind availability and discharging it during low wind periods. This not only reduces reliance on conventional generation but also enhances the overall reliability and cost-efficiency of the power system. Furthermore, the multi-period framework captures the temporal dynamics of wind generation and ESS operations, providing a realistic and robust optimization solution for renewable energy integration.

The study highlights the critical role of advanced optimization techniques, such as Multi-Period AC-OPF, in supporting the transition to sustainable and renewable energy systems. By leveraging ESS and optimizing renewable energy utilization, power systems can achieve greater operational flexibility and efficiency. Future research could explore the incorporation of other renewable energy sources, advanced ESS technologies, and stochastic modelling of uncertainties to further enhance the applicability and effectiveness.

REFERENCES:

[1] A. Meeraus A. Brooke, D. Kendrick, R. Raman, GAMS/Cplex 7.0 User Notes. GAMS Development Corp. (2000).

[2] A.J. Wood, B.F. Wollenberg, Power Generation, Operation, and Control (Wiley, Hoboken, 2012).

[3] P. Maghouli, A. Soroudi, A. Keane, Robust computational framework for mid-term techno economical assessment of energy storage. IET Gener. Transm. Distrib. 10(3), 822–831 (2016).

[4] F. Li, R. Bo Small test systems for power system economic studies, in: IEEE PES General Meeting (2010), pp. 1–4.

[5] R.D. Zimmerman, C.E. Murillo-Sanchez, R.J. Thomas, Matpower: steady-state operations, planning, and analysis tools for power systems research and education. IEEE Trans. Power Syst. 26(1), 12–19 (2011).

[6] A.J. Conejo, M. Carrión, J.M. Morales, Decision Making Under Uncertainty in Electricity Markets, vol. 1 (Springer, New York, 2010).

[7] F. Bouffard, F.D. Galiana, A.J. Conejo, Market-clearing with stochastic security-part II: case studies. IEEE Trans. Power Syst. 20(4), 1827–1835 (2005)

[8] A.M.Gee,F.Robinson,W.Yuan,Asuperconductingmagneticenergystorage-emulator/battery supported dynamic voltage restorer. IEEE Trans. Energy Convers. 32(1), 55–64 (2017)

[9] J.M. Lujano-Rojas, R. Dufo-Lpez, J.L. Bernal-Agustn, J.P.S. Catalo, Optimizing daily oper ation of battery energy storage systems under real-time pricing schemes. IEEE Trans. Smart Grid 8(1), 316–330 (2017).

[10] S. Pulendran, J.E. Tate, Energy storage system control for prevention of transient under frequency load shedding. IEEE Trans. Smart Grid 8(2), 927–936 (2017)